Donders Graduate School for Cognitive Neuroscience

Master of Science Programme

MSc Thesis

Hippocampus and human emotion control: a novel fMRI sequence shows hippocampal contribution within the Approach-Avoidance Task.

Author:

Gregorio Borghi

Supervised by:

Prof. Dr. Ivan Toni

Student name: Gregorio Borghi

Student Number: s1034199

Abstract

The hippocampus has been consistently implicated in spatial navigation and memory consolidation. Recently, anterior hippocampal sub-fields CA1 and CA3 have been involved in emotional action tendencies, like approach and avoidance behaviour. However, it remains unclear whether those sub-fields are also involved in supporting control over those emotional action tendencies. To study what neurophysiological substrates is involved in emotion regulation, which is the ability to control impulsive reactions, traditionally the approach-avoidance task (AAT) has been employed. Although the emotion control literature has shown network of different brain areas interacting when participants had to control their emotions, those studies could not test whether CA1/CA3 was part of the emotion control brain network. The current study tests this possibility, using a novel flow-sensitive high resolution fMRI sequence in thirty-eight participants performing AAT, a task where participants approached or avoided visually displayed emotional faces (happy or angry) by pulling or pushing a joystick. Approaching angry and avoiding happy faces (incongruent condition) requires rapid application of cognitive control to override prepotent habitual action tendencies to approach appetitive or to avoid aversive situations. A ROI analysis was employed, encompassing the the anterior prefrontal cortex (aPFC), amygdala (BLA), and anterior hippocampus. Moreover, single-subject beta values were extracted from peak-voxel CA1 and CA3 and were analysed through a Bayesian statistics. Results showed replication previous findings for the aPFC and BLA, hence validating the sensitivity of the novel fMRI sequence. However, single-subject beta-values analysis did not confirm the presence of neither CA sub-fields contribution within AAT. Despite such findings, results at the group level show congruency-related activation within the anterior hippocampus, hence potentially revealing small and distributed anterior hippocampal contribution in the emotion regulation network.

Introduction

In everyday life, individuals encounter objects or situations, such as a venomous spider, a cute puppy, or even another person, which can trigger impulsive reactions. The ability to control those impulses to behave in accordance with the environmental demands or personal goals is key for survival. Such an ability has been called emotion control and it has had a surge of interest within the Social Neuroscience field in the last years, both from the neurodevelopmental perspective (Chang et al., 2015; Tyborowska et al., 2016) to the departure from neurotypical functioning in clinical disorders (Joormann & Gotlib, 2010; Kaldewaij et al., 2019a; Volman et al., 2016). Neuroscientific research within this field has uncovered different brain areas acting as an interconnected network when participants must exert emotion control skills (Volman et al., 2011, 2013). Three key structures have emerged: the anterior prefrontal cortex (aPFC), the posterior parietal cortex (PPC), and the amygdala. More specifically, what has been consistently found in the literature is an up-regulation of the former two structures, whilst a down-regulation of the amygdala. Volman and colleagues explained such results by the inhibiting role that the aPFC has over the erupting automatic response processed in the amygdala, further up-regulating regions involved in rule and behaviour selections (PPC). However, limited statistical sensitivity and relatively coarse anatomical resolution might have prevented the detection of other brain regions involved in the control of emotional tendencies. For instance, recently Bramson et al., (2018) showed in an electrophysiology-based study the activation of the sensory-motor cortex (SMC), hence adding the motor initiator component to the emotion control network.

Such a finding suggest that additional but previously undetected structures might be implicated within this functional network that would further explain the neuro-mechanisms that govern emotion control. For instance, a possible candidate is the anterior hippocampus, and there are several motivations why that would be the case. First, the hippocampus is a structure closely connected to both amygdala and aPFC (Karalis et al., 2016; Pitkänen et al., 2000; Stein et al., 2007; Tzschoppe et al., 2014), which also displays similar neurophysiological features to what has been observed in the emotion control research, such as oscillatory theta modulation (Bienvenu et al., 2012). Secondly, the hippocampus has been shown to contribute to non-social approach-avoidance behaviour in conflict-based tasks in mice (Ito & Lee, 2016; Schumacher et al., 2016). In fact, mice displayed opposite activation in sub-nuclei CA1 and CA3 depending on whether the mice were approaching or avoiding the stimulus (Schumacher et al., 2018). Further, hippocampal activation has been observed in inhibitory response control during cue competition (Ito & Lee, 2016), monitoring threat levels (Bach et al., 2014, 2019) and threat-features such as probability and magnitude of threats (Abivardi et al., 2020). Finally, it is likely that methodological limitations caused by the employment of classical fMRI sequence (e.g., signal drop-out due to strong field inhomogeneity in the Medial Temporal Lobe) or methodological choices, such as applying only congruency contrasts, might have led to missing weak yet important hippocampal activation.

Therefore, this study aims to increase the current understanding of how emotion control is implemented in the human brain, specifically by investigating whether the hippocampus has a significant contribution within the

emotion control network in a neurotypical adult population using the Approach Avoidance Task (AAT). To overcome the methodological limitation caused by standard fMRI sequences, the study will employ a novel fMRI sequence called Arterial Blood Contrast (ABC) (Schulz et al., 2020). This novel sequence allows for reducing time to echo (TE) and so potential signal drop-out in the Medial Temporal Lobe, hence increasing the signal coming from that brain region. However, since this fMRI sequence has remained largely untested aside from visual cortex-based research (Schulz et al., 2020), this study will also seek further experimental validity for such a sequence in a different experimental set-up. Validation of the ABC sequence will involve replication of previous findings, specifically showing involvement of the aPFC and the amygdala within the AAT (Bramson et al., 2020; Kaldewaij et al., 2019a; Roelofs et al., 2009; Volman et al., 2011, 2013, 2016). Moreover, to verify whether CA1 and CA3 hippocampal sub-fields have opposite activation for approaching and avoiding behaviour, we will focus on approach and avoidance responses, irrespectively of emotional congruency effects. According to the previous literature, we expect the opposite activation within CA1 and CA3, the former being up-regulating for approach behaviour whilst the latter for avoiding behaviour (Schumacher et al., 2018).

Methods

Participants

Although the total amount of participants recruited for this study were 45, the final analysis comprised 38 participants since 7 participants had to be removed due to technical issues (n= 3) or inadequate task performance (n= 4). All participants had normal or corrected-to-normal vision and were right-handed, in addition to presenting no previous brain surgery, suffering from any brain-related illnesses, or psychiatric disorders (further demographic details are presented in table 1). Participants were recruited through the online system SONA, excluding participants with a body mass index (BMI) outside the healthy cohort (18-25 BMI) to avoid exceeding guidelines for specific absorption rate (S.A.R.) during MR scanning. Before signing the consent form, participants were informed about the risks and then details of the experimental procedure. The study falls under general ethics approval (CMO 2014/288) following the Declaration of Helsinki.

Table 1: The mean and standard deviation of Participants' age and hormonal levels, testosterone and cortisol before (T1) and after fMRI (T2), are displayed.

	Age	**Testosterone T1 (pg/ml)**	**Testosterone T2 (pg/ml)**	**Cortisol T1 (nmol/l)**	**Cortisol (T2) (nmol/l)**
Male Participants (n=15)	27.8 (1.88)	64.94 (4.86)	69.53 (4.92)	4.68 (0.52)	4.1 (0.6)
Female Participants (n=23)	24.52 (0.68)	20.55 (1.14)	15.16 (0.86)	8.72 (2.12)	5.41 (1.05)

Experimental Paradigm

Participants performed an approach-avoidance task (AAT) administered through Presentation (Version 18.0, Neurobehavioral Systems, Inc., Berkeley, CA, www.neurobs.com) software in the MRI scanner and lasted on average 40 minutes. Prior the start of the AAT, joystick response parameter were calibrated. During the entire AAT procedure, the screen presented a black background, whilst black-and-white experimental stimuli and white-font instructions were placed in the middle of the screen. Trials started with presentation of a white fixation cross for 500ms, followed by real-human sad or angry face presented for 100ms. Face stimuli employed within the study were sampled from the Karolinska Institute (Roelofs et al., 2009, 2010; van Peer et al., 2007). After presentation of face stimulus, participants had a 2000ms time-window to respond by either pushing or pulling the joystick (visual representation of trial structure is displayed in figure 1). If participants failed to respond within such time-window, a written message would appear in the middle of the screen for

3000ms stating "response was too late"; at the end of the 3000ms and only if the joystick was replaced in baseline position, the next trial begun. If the joystick was not back to baseline, a written message appeared on the screen stating "please place joystick back in the middle" and the next trial would start only once the participants brought the joystick back to baseline position. Moreover, trials were divided by a 3000 to 5000ms interval, and the experiment comprised 288 trials divided in 24 blocks, each block with a total of 12 trials. Prior the start of each block, written block-instructions were displayed on the screen, informing participants to push or pull the joystick accordingly to what emotion was the face stimulus showing (i.e., happy or sad). The study presented a repeated-measures block-design, in which blocks equally alternated between two experimental conditions: congruent and incongruent. Within the congruent condition, participants had to respond in a manner that is congruent with the automatic movement reactions (i.e., approach/ "pull towards yourself the joystick" a positive stimulus vs avoiding/ "push away the joystick" a negative stimulus; Klein et al., 2011). Therefore, within the congruent condition, the joystick had to be pulled when observing a positive valence stimulus (e.g., a happy face) and pushed away if the stimulus was negatively valence (e.g., an angry face), whilst vice versa in the incongruent condition (schematic representation of possible valence-response combinations is depicted in figure 2).

INSERT FIGURE 1

Figure 1: visual example of the structure of a single trial in AAT.

Testosterone and Cortisol Sampling

Since previous research has shown that a significant part of participants' behavioural and neurophysiological variance within the AAT could be explained by endogenous testosterone and cortisol levels (Kaldewaij et al., 2019b; van Peer et al., 2007; Volman et al., 2016), those hormones were sampled through saliva at two separate time-points outside the MRI: before the experimental procedure (T1) and after its completion (T2). To avoid possible confounds, participants were asked not to eat or drink anything one hour before the start of the experiment. Saliva samples were collected by Salivette® (Sarstedt, Hildesheim, Germain). Due to possible hormone contamination from the researchers, participants were asked to open themselves the Salivette and keep in their mouth the biocompatible synthetic fibre roll without chewing it for four minutes. Then, participants were asked to put back the fibre roll into the Salivette, subsequently stored at -80°C. The Salivette of all participants were then sent in one batch to Dresden LabService GmbH for cortisol and testosterone analyses, which involved immuno-assay techniques. The results obtained from the immune-assay are shown in table 1. SPSS version 25 (IBM Corp., 2017, www.ibm.com) was employed to correlate time-1 (T1) and time-2 (T2) hormonal scores to check whether participants' hormonal levels were consistent throughout the experiment. In addition to the Pearson'scorrelation, a pair-wise t-test was employed to check consistency of hormonal levels. The results of the Pearson's correlation showed that T1-T2 hormonal levels were significantly correlated for both cortisol ($r_{(36)}=0.746$, $p<0.001$) and testosterone ($r_{(36)}=0.925$, $p<0.001$). However, since pair-wise Student's t-test showed a significant difference between T1 and T2 scores for cortisol ($t_{(36)}=2.205$, $p=0.034$) but not for testosterone ($t_{(36)}=0.537$, $p=0.595$), later analyses employed only T1 scores to avoid

possible task-related confounding effects over hormonal scores. Then, both testosterone and cortisol scores were log-transformed to ensure normal distribution and z-standardised within gender. T1 Hormonal scores were then used as covariates for both behavioural and neuroimaging data.

INSERT FIGURE 2

Figure 2: schematic representation of experimental conditions in AAT(obtained from Volman et al., 2011, 2013). The figure shows the possible configuration between participant's response and stimulus valence, which define whether the trial was affect-congruent or -incongruent.

Data Acquisition

Brain images were acquired in a single session using a 3T MAGNETOM Prisma MRI scanner (Siemens AG, Healthcare 152 Sector, Erlangen, Germany) using a 32-channel head coil. An EIKI LC- XL100 beamer 154 was used to display stimuli with a resolution of 1024 x 768 and a refresh rate of 60Hz projected on a screen behind the scanner bore. Participants used a mirror to look at the stimuli displayed and responded using a customised fibre optic response joystick that could only move in the sagittal axis.

The experimental procedure involved four different MRI sequences: auto-align head scout, functional ABC, T1-weighted image, and T2-weighted image. The auto-align head scout sequence was employed to align the field of view to a built-in brain-atlas, which allows acquisition of the field of view.

Arterial Blood Contrast (ABC) functional sequence:

After completion of the auto-align head scout sequence, the Arterial Blood Contrast (ABC) sequence was initiated. The ABC sequence was chosen due to a number of important characteristics that make it particularly interesting for studying subcortical areas such as the hippocampus or the amygdala. First, it allows to greatly reduce the TE parameter, thus preventing possible signal drop-out and spatial inaccuracies in sensitive areas such as the medial temporal lobe (Olman et al., 2009). This is possible because by employing magnetisation transfer (MT), the signal from the tissue saturates and attenuates, whilst the one from the blood is not affected (Balaban et al., 1991; Wolff & Balaban, 1989). Therefore, since brain activation leads to an increase in blood volume, we can observe an increase in signal intensity as well (Kim et al., 2008; Zhou et al., 2005). Finally, since the arteries and capillary vessels are the major contributors to blood volume change, it can be claimed that ABC records up-stream signal, differently from classic BOLD-based sequences that are sensitive to downstream signal (Schulz et al., 2020). Therefore, although the ABC sequence is novel and largely untested outside the visual cortex, it is better suited for the current experimental question. The acquired functional images had a single echo with TR= 2010ms, TE= 11ms, 48 slices, flip angle of 50°, GRAPPA-based acceleration factor of 3, slice orientation T > C, voxel size= 2 x 2 x 2mm, and phase encoding direction A >> P. In addition, the ABC sequence presented special (MT) parameters that were also applied to saturate the signal and measure changes in the cerebral blood volume: MR duration of 1500μs, 180° MT flip angle, and 1 slice skipped in TR.

High-definition Anatomical sequences:

T1-weighted high-resolution anatomical images were acquired using MPRAGE sequence with a GRAPPA-based acceleration factor of 2, TR= 2200ms, TE= 2.64ms, voxel size= 0.8 x 0.8 x 0.8mm, 224 slices in sagittal orientation, distance factor of 50%, A >> P phase-encoding direction, and FOV= 256mm.

Moreover, the study also employed T2-weighted anatomical image to improve the quality of anatomical segmentation of the hippocampus (Iglesias et al., 2015; Wisse et al., 2017; Yushkevich et al., 2015). Such images were acquired using a Turbo-Spin Echo (TSE) sequence that presented with TR= 5600ms, TE= 71ms, flip angle of 150°, voxel size= 0.4 x 0.4 x 2.0, 30 slices in transversal orientation, R >> L phase-encoding direction, FOV= 220mm. No acceleration and distance factors were employed for this sequence. Furthermore, the choice of employing such anisotropic voxel size was driven by the fact that the hippocampus presents much sharper structural changes in the coronal and sagittal axes, whilst not as much in the axial axis (Yushkevich et al., 2015). Therefore, to reach a much more accurate segmentation of hippocampal sub-fields, it was decided to employ a much higher definition in those two directions.

Behavioural Analysis

Participants' reaction time (RT) for correct responses and error rates were recorded. Both RT (*ms*) and error rate (*% of incorrect trials*) preprocessing were conducted in Matlab2020b (The Math Works, Inc., 2020, www.mathworks.com). Regarding reaction times preprocessing, blocks that presented more than 50% of incorrect trials were removed from the analysis of the behavioural data. Moreover, trials that presented either "too-late response" and/or joystick errors were also excluded from subsequent analysis. Furthermore, trials that displayed extreme responses (RT<500ms or RT>1500ms) or more than three standard deviations away from the grand participant average RT were excluded. Subsequently, RT data were log-transformed to ensure normal distribution. Regarding error rate, trials counted as errors were those that presented joystick errors and incorrect responses. Subsequent analyses employed gender as a between-subject variable and were conducted in JASP version 0.14.1 (JASP Team, 2020, https://jasp-stats.org/) since it allows Bayesian-based statistical methods.

The choice of employing Bayesian statistical methods was taken because it allows to measure the strength of evidence for both the null and the alternative hypothesis (Dienes, 2016). The study uses the statistical threshold suggested by Jeffreys (1939). In detail, the Bayes factor threshold is divided into three major bands: $BF_{10} > 3$ substantial evidence for the alternative hypothesis, $1/3 > BF_{10} > 3$ inconclusive evidence, $BF_{10} < 1/3$ substantial evidence for the null hypothesis. Furthermore, a Bayes factor was computed by dividing the posterior probability of the model with the posterior probability of the other remaining models, thus obtaining an indication of the amount of evidence favouring a specific model (Kass & Raftery, 1995). Moreover, we also obtained in single effect's probability by marginalisation. The detail regarding Bayesian statistics also applied for the neuroimaging-based inferential statistics, which are later described. Moreover, the statisical models

employed in the Bayesian mixed-factor ANOVA for both behavioural and neuroimaging statistics are present in Appendix 1.

Pre-processing

Brain data were pre-processed using the Matlab toolbox SPM12 v7771 (Statistical Parametric Mapping, 2014, www. fil.ion.ucl.uk/spm). First, functional neuroimaging data were rigidly realigned using a least-square approach and employing six rigid-body parameters for spatial transformation. As reference image for the realignment step, the first functional image was chosen. Subsequently, since the sequence presents a TR>1800ms, slice time correction was performed. In detail, the 1st slice (0.995*s*) was chosen as reference since it was the slice that was closest to half of the TR (2.01*s*). Once slice time correction was completed, functional and anatomical images were co-registered to the mean of the functional image, which was created just before co-registration. Once co-registration was completed, normalisation of both functional and anatomical T1-weighted and T2-weighted images was initiated. We re-sampled the functional images to 0.8mm isotropic resolution, to match the resolution of the T1 anatomical image and differentiate hippocampal sub-fields activity. Normalisation maintained the original voxel size for both T1-weighted anatomical images (isotropic 0.8mm) and T2-weighted (anisotropic 0.4x0.4x2mm). The normalisation step employed non-linear image registration of all functional and anatomical images to Montreal Neurological Institute (MNI) template. After normalisation, T1-weighted anatomical images were segmented into white matter (WM), grey matter (GM), and cerebral spinal fluid (CSF). Co-registration of the normalised images was checked and another co-registration step was employed if necessary. Functional images were spatially smoothed with a FWHW Gaussian kernel of 4mm.

Hippocampal Segmentation

The software employed for hippocampal segmentation was FreeSurfer 7.1.1 (http://surfer.nmr.mgh.harvard.edu/). The choice of FreeSurfer for this study was driven by the fact that it employs a complete automatised algorithm without the need for any manual intervention, which is employed by other segmentation mixed automatised-manual approaches such as ASHS (Yushkevich et al., 2015). The study employed 2mm isotropic functional images in addition to 0.8mm isotropic anatomical images and a dedicated T2-weighted anatomical image, hence significantly increasing confidence of correct segmentation implementation (Iglesias et al., 2015). Furthermore, new longitudinal evidence also shows FreeSurfer's high test-to-test reliability across time and across scanner, which also increased confidence for correct segmentation (Brown et al., 2020).

The segmentation pipeline started with applying the "*recon-all*" (Dale et al., 1999; Dale & Sereno, 1993; Fischl et al., 2001, 2002; Fischl, Salat, et al., 2004; Fischl, Sereno, & Dale, 1999; Fischl, Sereno, Tootell, et al., 1999; Fischl, van der Kouwe, et al., 2004; Fischl & Dale, 2000; Han et al., 2006; Jovicich et al., 2006; Reuter et al., 2010; Ségonne et al., 2004) algorithm of the normalised T1-weighted image to obtain a first structural analysis

of participants' anatomical image. A normalised T2-weighted image was converted into mgz format by "*mri_convert*" (http://surfer.nmr.mgh.harvard.edu/) algorithm. Subsequently, the segmentation was applied by "segmentHA_T2" (Iglesias et al., 2015; Saygin et al., 2017) algorithm, allowing the creation of both hemispheres amygdala and hippocampal sub-fields. Once those were obtained, the left and right hemispheres file were joined together and separate subject-specific masks for anterior-only CA1 and CA3, and BLA (N.B. BLA masks included also Accessory BLA nucleus) were created through "*mri_binarize*" command. Moreover, single-subjects' anterior CA1 and CA3 masks were joined together by "*fslmaths*" algorithm (Jenkinson et al., 2012) to create single-subjects anterior-CA masks. Then, "*fslmaths*" was employed again to combine single-subjects CA masks to each other, hence creating a more anatomically-precise group masks compared to masks obtained from general anatomical atlases, since it encompasses only anterior hippocampal areas (illustrative example of single-subject segmentation, group-level CA mask, and AAL-based hippocampal mask is available in figure 3). The same procedure was applied for BLA group-level masks.

First & Second-Level Analysis

Single-subject and group-level analyses of functional images were conducted on SPM12 Matlab toolbox and following the pipeline used in Tyborowska et al. (2016). A general linear model was employed to analyse functional activation. The study used an event-related design, hence the single-subject analysis employed a design matrix that presented regressors describing the onset and duration of each trial for the four experimental conditions (i.e., approach-happy, approach-angry, avoid-happy, avoid-angry). In addition to these, the design matrix contained a regressor for misses, if response was incorrect or too late, and presentation and duration of block instructions. The six regressors were then convolved with a canonical haemodynamic response functions. Moreover, to account for in-scan head-movements, the design matrix employed nuisance regressors obtained by computing the linear, quadratic, cubic, first- and second-order derivatives of head-movement parameters, which were collected from the realignment step during the preprocessing (Lund et al., 2005). Last, the design matrix employed three additional regressors representing the signal intensity time-course of WM, GM, and CSF. The employment of these three additional regressors aimed to account for image intensity shifts that might result from hand -movements within the magnetic fields of the MRI (Verhagen et al., 2006). The last step of first-level analysis involved high-pass filtering with a 128s cut-off of the fMRI time series. To account for temporal autocorrelation and white noise, "SPM FAST" algorithm was employed (Luo et al., 2020).

The second-level analysis employed a random-effects multiple regression analysis over the contrast images of the effects of interests, which are the previously-mentioned experimental conditions. Participants were divided according to gender, and hormonal scores for both cortisol and testosterone were log-transformed and standardized per gender. Since previous studies have shown the impact of both hormones in this experimental set-up (Kaldewaij et al., 2019a; Volman et al., 2011), hormonal scores were added covariates for subject, group, and condition. Since the current study employs a novel fMRI sequence, to test the efficacy of ABC sequence the study aims to replicate the basic congruency effects that have been consistently found during the AAT performance within the aPFC and the amygdala. Furthermore, if those effects were found, it would

provide further robustness over potential hippocampal results. Whilst the ROI-masks for the anterior CA and basolateral nuclei were obtained from FreeSurfer segmentation, to maintain consistency with previous AAT studies the aPFC mask that was employed was taken from Neubert et al., (2014) parcellation. Statistical inferences on aPFC and amygdala effects were made over group-level data, within each ROI, at voxel-level $p_{FWE} < 0.05$. The same analysis was also repeated by employing group-level hippocampal mask, since it allows for testing congruency effect within the entirety of the anterior hippocampal area, hence checking for significant AAT-related activation in sub-fields outside the CA1 and CA3 areas.

Statistical inferences on CA1 and CA3 were made according to the following procedure. Within each participant-specific ROIs in CA1 and CA3, we identified the local maximum from the F-contrast of the difference between approach and avoid responses. The participants' beta-values from the four experimental conditions (approach-happy, approach-angry, avoid-happy, avoid-angry) were entered in a Bayesian-based four-way mixed-measures ANOVA, which presented three repeated-measure variables (Factor 1: Response, with two levels - approach and avoid; Factor 2: Valence, with two levels - happy, angry; Factor 3: Region, with two levels - CA1, CA3) and one between-subject variable (Factor 4: Gender, with two levels - male, female). The ANOVA also included cortisol and testosterone scores as covariates. This statistical approach was chosen since it allows for testing the hypothesis of a differences in the contribution if CA1 and CA3 to approach and avoidance response (Abivardi et al., 2020; Schumacher et al., 2018) and whether CA presents a congruency effect similar to either the aPFC or the amygdala.

INSERT FIGURE 3

Figure 3: Illustrative examples of the brain mask created and employed in the study. **A)** Single participant's hippocampal and amygdala segmentation, displaying the resulting amygdalo-hippocampal sub-subfields that can be obtain through FreeSurfer. **B)** Single-subject frontal CA1 (yellow) and CA3 (red). **C)** Group-level CA mask created by super-positioning of all participants' frontal CA1 and CA3. **D)** Hippocampal mask obtained from the AAL atlas (SPM12)

Results

Behavioural Results

The descriptive regarding the behavioural results are depicted in figure 4. Furthermore, all effect and interactions are present in appendix 2, whilst below are only described the effect and interaction of interest.

INSERT FIGURE 4

Figure 4: Participants' reaction times (**A**) and error rates (**B**) average for the four experimental conditions are displayed. Black lines represents the mean (continuous lines) and the standard error of the mean (dotted lines).

Regarding RT scores, the analysis showed the absence of evidence for all factors and their interaction within the mixed-measures ANOVA. For instance, of the three main effects fed into the analysis, there was strong evidence for absence of an effect for both valence (BF_{incl}= 0.033) and response (BF_{incl}= 0.027). Moreover, RT also showed strong evidence for absence of a congruency effect (*response*valence:* BF_{incl}= 0.008) or any other interaction.

On the other hand, error rate scores displayed a different kind of portrait compared to RT. It is important to mention that four participants were excluded from the error-rate analysis since they presented an error-rate score more than three standard deviations away from the group-level average. Specifically, whilst the evidence in favour for valence (BF_{incl}= 0.713) and response (BF_{incl}= 0.659) factors resulted inconclusive, there was moderate evidence in favour for the presence of a gender-effect (BF_{incl}= 6.515) and for a congruency-effect interaction (*response*valence*: BF_{incl}= 3.571). Therefore, the data shows the existence of a difference between males and females, with females making less mistakes than males, and between congruent and incongruent trials, the latter showing a higher error rate. However, all other factors and interactions showed substantial evidence for the null hypothesis, hence not playing a role in potential differences in error rates among groups and trials.

Single subject-level fMRI

The first step of this analysis stage was to explore whether human hippocampal sub-fields' (CA1 and CA3) peak voxel's beta values were consistent with the animal research findings. The distribution of the evidence for all factors and their interaction within the four-way mixed-effects ANOVA showed either inconclusive evidence or absence of an effect within the data. For instance, whilst the beta values showed inconclusive results for response factor (BF_{incl}= 0.953), data distribution resulted in strong absence of an effect for CA (BF_{incl}= 0.044) or the interaction between the CA and Response factors (*response*CA*: BF_{incl}= 0.033). In addition to that, the evidence for the congruency effect interaction also showed absence of an effect (*response*valence*: BF_{incl}= 0.097). Moreover, the addition of gender (*response*valence*gender*: BF_{incl}= 0.125) or CA (*response*valence*CA*: BF_{incl}= $7.525e^{-4}$) or both (*response*valence*gender*CA*: BF_{incl}= $1.795e^{-5}$)

factors within the interaction biased the Bayesian Factor towards even stronger evidence for absence of an effect.

Group-level fMRI

The summary of the results for the fMRI ROI analysis at the group-level is shown in table 2, whilst the depiction of testosterone modulation over the different ROIs is illustrated in appendix 3. Visual illustration of ROI activation for aPFC, BLA, and CA masks is showed in figure 5.

Table 2 Significant voxels found in the ROI analyses showing congruency effect within AAT

Anatomical Region (Mask)	**Hemisphere**	**MNI Coordinates**			p_{fwe}	Z_e	**t**
		X	**Y**	**Z**			
Increased activity - Congruency effect							
Lateral Frontal Pole	R	20.4	63.2	10.8	.001	5.47	5.94
	L	-27.6	50.4	3.6	.027	4.60	4.88
Decreased Activity - Congruency Effect							
Lateral Frontal Pole	R	18.8	55.2	-4.4	.001	5.40	5.85
BLA	R	35.6	52	2	< .001	5.31	5.74
Anterior Hippocampus	R	26	-4.8	-21.2	< .001	4.36	6.00
Positive Testosterone Modulation of Congruency							
Lateral Frontal Pole	L	-26	53.6	-14.8	.009	4.87	5.20
	R	14.8	64.8	0.4	.042	4.49	4.75
BLA	L	-18.8	-2.4	-14.8	.014	4.36	4.59
Anterior Hippocampus	L	-23.6	-17.6	-15.6	.005	4.74	5.04
	R	28.4	-12.8	-14.8	.026	4.34	4.58
Negative Testosterone Modulation of Congruency Effect							
Lateral Frontal Pole	R	35.6	52	2	.001	5.28	5.70
	L	-25.2	47.2	-0.4	.016	4.73	5.03

Anterior Hippocampus	L	-29.2	-8.8	-29.2	.013	4.51	4.92
	R	25.2	-12.8	-14.8	.026	4.34	4.78

Regarding the lateral frontal pole (lFP), significant activation was found when different contrasts were applied. For instance, two voxels ([20.4, 63.2, 10.8]; [-27.6, 50.4, 3.6]) show significant congruency effect, whilst a different voxel ([18.8, 55.2, -4.4]) show significant opposite activation, hence higher activation during congruent trials. On the same line, the analysis also showed dual-directional significant testosterone modulation, displaying positive and negative modulation.

A similar trend was found in the anterior hippocampal area, showing significant deactivation during incongruent conditions in one voxel ([26, -4.8, -21.2]), and dual directionality for testosterone modulation.

The last ROI that was examined was the basolateral nuclei of the amygdala (BLA), which showed a significant decrease of activity for the congruency effect within one voxel ([35.6, 52, 2]). In addition to this, testosterone was found to have a positive modulatory effect for congruency effect in one voxel ([-18.8, -2.4, -14.8]) located in the BLA.

INSERT FIGURE 5

Figure 5: visual representation of masked above-threshold (p< .0.001) group-level activation for the three regions of interest. **A)** Main task effects for incongruent > congruent within the aPFC. **B)** Main task effects for congruent > incongruent within the BLA. **C)** Main task effects for congruent > incongruent within the anterior hippocampal sub-fields.

Discussion

The current study had a dual aim: first, it intended to study the presence of hippocampal CA sub-fields contribution within approach-avoidance response during AAT, theorising a specific directionality of such contribution: CA1 for approach response and CA3 for avoid response. Second, the study attempted to address its primary goal by employing a new experimental fMRI sequence (i.e., ABC), hence seeking further experimental validity outside the previously tested visual domain. In detail, the study sought to accomplish its second goal by replicating the previous findings within the AAT literature, thus testing the presence of a congruency effect within the aPFC and the amygdala. The group-level results from the ROI analysis confirmed the typical congruency results, thus an up-regulation of the aPFC and a down-regulation of the amygdala during incongruent trials when compared to congruent trials. Last, the BLA shows positive modulation driven by participants' testosterone levels, which could potentially signify higher amygdala activation in those who had a higher levels of testosterone, which is also in line with previous research (Volman et al., 2011, 2013). However, to confirm this latest hypothesis, more analysis should be run. In summary, regarding the second goal of the study, we can safely claim that the validity ABC sequence has been confirmed within the social neuro-cognitive domain tackled by the AAT. However, in addition to these findings, the results have shown

activations that are in contrast with the AAT literature, which will be later discussed more in detail. Moreover, the behavioural results were also in line with previous studies, although they showed a congruency effect for error rates whilst no effect for reaction times, which is the opposite of what has been traditionally observed (Volman et al., 2011, 2013).

The confirmation of the ABC validity has allowed us to verify hippocampal contribution with more confidence; specifically, we investigated whether CA1 and CA3 have opposite activation for approach and avoid responses despite the valence of the stimulus, which is what appears within approach-avoid conflict (AAC) literature (Schumacher et al., 2016). The study employed Bayesian-based methods, hence allowing to test the amount of evidence favouring both the alternative and the null hypothesis (i.e., H0>H1 or H0<H1). The distribution of the extracted beta values from the single-subject peak-voxel within CA1 and CA3 showed no difference from the predicted null-hypothesis distribution. Therefore, we had to accept the null hypothesis, which claimed that hippocampal sub-fields CA1 and CA3 had no differential activation for approach or avoid responses. Furthermore, we investigated whether the same most active CA1 and CA3 voxels showed congruency effect, although this time we did not specify the direction (i.e., either up- or down-regulation). We obtained similar results to the previous analysis, observing strong evidence favouring absence of a congruency effect, hence we had to accept the null hypothesis. Finally, post-hoc analysis over second-level fMRI analysis employing the group-level hippocampal mask has shown novel and unexpected results. In fact, even though there was a down-regulation during incongruent trials within one hippocampal voxel, the results showed both positive and negative modulation of testosterone over different voxels present in the hippocampus. All these results will be further discussed.

Replication of previous results

One of the goals of the present study was to validate the ABC sequence by replicating the traditional results obtained in AAT. It is important to remind that testosterone was normalised across gender, hence making males' testosterone levels comparable to those in females. Although the replication was successful (i.e., congruency effect in aPFC and amygdala), few aspects need further discussion. For instance, it is important to mention that we were not able to observe Parietal cortex activation during the AAT since this area was placed outside the field of view (FOV) of the sequence. The decision of excluding the Parietal cortex was obliged by the need of decreasing the voxel size from 3mm isotropic to 2mm isotropic without having to change any of the MRI-related parameters, especially the TE since its shortness was the main advantage of ABC sequence. The choice of employing a 2mm isotropic voxel was driven by the desire of studying the hippocampal CA sub-fields, which are extremely small and so required as small of a voxel as possible. However, by excluding the parietal cortex the study excluded the possibility of examining PPC and SMC, which are also key structures within the AAT framework (Bramson et al., 2018; Volman et al., 2011).

Furthermore, although the study replicated AAT congruency-related results, it has also found activation in conditions that traditionally have not been found in the AAT. For instance, one voxel in the aPFC was found more active during congruent trials compared to incongruent ones. Although this findings are clearly in contrast with the previous studies, there can be different causes that could potentially explain such contradicting finding. First, differently from previous studies, we decided to up-sample functional images from 2mm to 0.8mm, which allow a much higher spatial definition at the expense of signal strength. Although this choice was made with the purpose of studying the hippocampal sub-fields, it might have brought important consequences in the other ROI-based analyses, such as revealing not-hypothesised heterogeneous activation. For instance, it has been shown that the aPFC can be a highly heterogeneous area (Toro-Serey et al., 2020), hence it is possible that employment of smaller voxel size have been able to disclose such functional heterogeneity, which might have been averaged out by employment of larger voxel size within previous studies. This view would be further confirmed by the presence of dual-directional modulation of testosterone in the aPFC, showing heterogeneous activity within this region. In fact, the study also showed a positive and negative modulation of the aPFC driven by testosterone levels, which even though is in line with previous developmental findings (Tyborowska et al., 2016), it has not been found in adult participants. However, as shown in Tyborowska and colleagues (2016), the presence of testosterone might be linked with organisational and cognitive control functions, the former slowly decreasing with age maturation. Such a hypothesis is compatible with our findings since human adult's aPFC has shown maturational changes up until the late 20s (Fuster, 2002; Giedd et al., 1999). Therefore, it is possible that not all participants within the study might have presented a fully matured aPFC, which would explain the positive testosterone modulation, whilst for those who did present a matured aPFC, testosterone would become detrimental for cognitive control, thus explaining the negative modulation. However, to draw stronger conclusion further analyses are needed.

Moreover, differently from previous research, this study has tested all directional congruency contrasts for all regions, also those that were not classically tested such as higher activation for congruent trials in the aPFC or higher activation for incongruent trials within the BLA. Although it is not wrong to employ only theory-driven contrasts, especially if the amount of evidence is particularly strong such as in AAT literature (Bramson et al., 2018, 2020; Kaldewaij et al., 2019b; Roelofs et al., 2009; Volman et al., 2011, 2013), there is a consistent risk of ignoring theory-incongruent yet statistically significant activation, which is what the current study has unveiled. Therefore, even though there is a considerable amount of AAT-related studies, these results suggest to future research to include in their ROI-based analysis both directional contrasts for all brain masks to avoid missing important brain activation.

CA1 and CA3

The evidence obtained by single-subject peak voxel's beta values clearly favours the null hypothesis, hence that CA1 and CA3 sub-fields show neither response preference (i.e., approach and/or avoid) or congruency effect. This finding is in contrast with what animal and human research have shown in the past within the AAC paradigm, even though there is one key difference between the current AAT and AAC domains. In fact, whilst

the AAC presents an approach-avoidance decision-based task within the context of reward, the AAT does not include any type of reward. In fact, within the AAC the human or animal subjects have to decide whether they want to make an approach response towards a rewarding stimulus (e.g., money or food) with varying degrees of risk of incurring into a negative stimulus (e.g., loss of money or electrical shock). Within these conditions research has shown hippocampal contribution for approach and avoid response in the CA1 and CA3 accordingly. On the other hand, even though within the AAT experimental set-up there is still an approach-avoid response, the clear difference from the AAC is that there is no clear positive or negative reinforce stimulus. In fact, the AAT employs faces to induce a natural approach and avoidance reaction, theorising the aPFC as the putative inhibitory structure (Volman et al., 2011), which is in contrast with the AAC literature that claims that hippocampus should be the inhibitory structure (Schumacher et al., 2016). Therefore, it is possible that the hippocampus CA sub-fields might have such an inhibitory role and codify for an approach-avoid response only within a reward-based environment whilst showing superfluous activity within a non-reward domain, such as the AAT. This hypothesis is further supported by animal model research specifically focusing on reward (LeGates et al., 2018; Schmelzeis & Mittleman, 1996; Sosa & Frank, 2018) that has shown a hippocampal connection with the reward network and the presence of a specific CA1 reward-computing neuropopulation. Moreover, the absence of a congruency effect in either direction (i.e., up- or down-regulation during incongruent trials) also further confirms the absence of Ammonis Corn's consistent contribution within the AAT.

Group-level hippocampal mask

Although the current study showed no significant contribution of the CA sub-fields within the AAT, group-level hippocampal analysis has shown one voxel being significantly more active for congruent than incongruent trials. This is particularly important because it shows that it is possible that other sub-fields outside the CA areas might still be implicated within AAT social processing. In fact, even though the group-level mask was created by summing normalised single-subject CA1 and CA3 masks together, due to idiosyncratic differences in brain shape still present and the small size of the different hippocampal sub-fields, the hippocampal mask encompassed several other hippocampal sub-regions outside the CA area (figure 3). Furthermore, this procedure has also allowed obtaining a much more precise hippocampal mask compared to a general mask obtained from atlases. Therefore, whilst single-subject results clearly show no implication of the CA sub-fields, it is possible that other hippocampal sub-fields might be involved in social-based neuro-cognitive phenomena. Such a hypothesis is further confirmed by the presence of both positive and negative testosterone modulation within congruency, confirming the presence of a heterogeneous hippocampal activity during AAT. The robustness of this finding is also supported by the presence of androgen receptors within the hippocampus, making a direct modulation of testosterone over this brain structure possible (MacLusky et al., 2006). However, it is impossible from this study to determine the exact role of such hippocampal contribution within the social domain tackled by the AAT, although we might guess few possibilities. For instance, it has been previously shown that the hippocampus has an important role in the recognition of social cues (Laurita

& Spreng, 2017), in retrieving social memories (Montagrin et al., 2018), and in ensuring social flexible behaviour (Rubin et al., 2014). All the processes are fundamental for the correct performance of AAT since participants must recognise face cues to deduct the stimulus' valence, retrieve socially relevant information, and control automatic responses.

Although hippocampal activation might appear too little within this study to claim a major role within the AAT congruency network, it might also be hypothesised a general secondary support role for correct network performance. For instance, specific hippocampal sub-fields might help to retrieve social cues (Laurita & Spreng, 2017) for more proficient valence-based amygdala processing (Conty & Grèzes, 2012; Muscatell et al., 2009), which would explain the higher hippocampal activation during congruent trials. However, it is also possible that the hippocampus might contribute in parallel yet simultaneous ways towards the emotion control network. Such an hypothesis would be supported by the presence of both positive and negative testosterone modulation over hippocampal congruency score. For instance, a higher level of testosterone within the hippocampus might result in cue retrieval impairment (Harooni et al., 2008), but it might also result in stronger social flexible behaviour (Rubin et al., 2014). However, additional complementary data should be collected and further analysis should be run before being able to draw any substantial claim.

Limitations

The study here presented employed several new methods to obtain novel research findings, showing both great methodological advancement, but also limitations that should be taken into account for future studies. For instance, since ABC is a CBV-based fMRI sequence, the study decided to employ a longer version of the AAT to increase the number of data points to compensate for the diminished signal that is obtained in comparison to BOLD-based sequences (Lu & van Zijl, 2012). However, by doing so the study did not take advantage one of the most important aspects of ABC, which is the possibility of employing a BOLD-based sequence as an additive signal for the CBV, as it was shown by Schulz et al. (2020). Therefore, it might be beneficial for future studies to employ a shorter version of the task, so that it can be repeated twice, and integrate the results of the two: once with ABC sequence and once with a BOLD-based sequence. Furthermore, the effects of the lower signal obtained by the fMRI sequence might have been exacerbated by voxel up-sampling during the normalisation step, bringing voxel size from 2mm to 0.8mm. As mentioned before, this was done to better investigate hippocampal sub-fields, but it had a dual negative effect. First, by diminishing voxel size, the already-low signal coming from the voxel was even more decreased; second, the amount of voxel dramatically increased, thus statistical analysis employing multiple comparison correction was also seriously affected (i.e., family-wise error correction). Regarding the statistical-base limitation, we tried to compensate for such a down-fall by employing Bayesian analysis over peak-voxel, disregarding whether such voxel was statistically significant, and employing evidence-based statistics and not frequentist-based one. However, in regard to diminished signal, nothing could have been done in that regard. Thus, it is possible that the low amount of significant activation in voxels and clusters found in this study might have been due to very low signal levels.

Therefore, if it is not possible to use a BOLD-based sequence in addition to the ABC, future studies might want to consider employing higher field strengths.

Future Directions

The results of the current study have shown the potential of ABC sequence to investigate areas that show high gradient susceptibility and signal drop-out, such as the medial temporal lobe. ABC has a huge potential for studying such difficult-to-image brain regions, and if summed with more classical methods such as BOLD-based imaging techniques, then the two techniques will be able to compensate each other disadvantages: lower but more localised signal from the ABC, stronger signal but more sensitive to signal drop-outs from the BOLD.

Regarding the results concerning hippocampal involvement within the AAT, future studies might want to investigate what hippocampal sub-fields outside the Cornus Ammonis area is involved within the emotion control network. In addition, further connectivity analysis might also give a better idea of what exact role the anterior hippocampus might have in controlling emotional responses. Such an investigation topic is not solely important for the emotion control field, allowing to expand and improve an over-simplified brain network, which is what this study has shown, but it also has other potential benefits. For instance, a better understanding of sub-cortical areas can have the beneficial effect of expanding and already-existing neuro-physiological intervention employing neuromodulatory techniques (e.g. Transcranial Ultrasound Stimulation) that aim to recalibrate over- or under-active brain regions. Last but not least, future studies investigating the hippocampus and/or the amygdala should start employing FreeSurfer-segmentation-based masks since it allows to create much more defined and participant-specific masks compared to mask created from brain atlases (figure 3).

References

Abivardi, A., Khemka, S., & Bach, D. R. (2020). Hippocampal representation of threat features and behavior in a human approach-avoidance conflict anxiety task. *The Journal of Neuroscience*, *40*(35), JN-RM-2732-19. https://doi.org/10.1523/jneurosci.2732-19.2020

Bach, D. R., Guitart-Masip, M., Packard, P. A., Miró, J., Falip, M., Fuentemilla, L., & Dolan, R. J. (2014). Human hippocampus arbitrates approach-avoidance conflict. *Current Biology*, *24*(5), 541–547. https://doi.org/10.1016/j.cub.2014.01.046

Bach, D. R., Hoffmann, M., Finke, C., Hurlemann, R., & Ploner, C. J. (2019). Disentangling Hippocampal and Amygdala Contribution to Human Anxiety-Like Behavior. *The Journal of Neuroscience : The Official Journal of the Society for Neuroscience*, *39*(43), 8517–8526. https://doi.org/10.1523/JNEUROSCI.0412-19.2019

Balaban, R. S., Chesnick, S., Hedges, K., Samaha, F., & Heineman, F. W. (1991). Magnetization transfer contrast in MR imaging of the heart. *Https://Doi.Org/10.1148/Radiology.180.3.1871277*, *180*(3), 671–675. https://doi.org/10.1148/RADIOLOGY.180.3.1871277

Bienvenu, T. C. M., Busti, D., Magill, P. J., Ferraguti, F., & Capogna, M. (2012). Cell-Type-Specific Recruitment of Amygdala Interneurons to Hippocampal Theta Rhythm and Noxious Stimuli In Vivo. *Neuron*, *74*(6), 1059–1074. https://doi.org/10.1016/j.neuron.2012.04.022

Bramson, B., Folloni, D., Verhagen, X. L., Hartogsveld, B., Mars, R. B., Toni, X. I., Roelofs, X. K., Verhagen, L., Hartogsveld, B., Mars, R. B., Toni, I., & Roelofs, K. (2020). Human Lateral Frontal Pole Contributes to Control

over Emotional Approach–Avoidance Actions. *The Journal of Neuroscience*, *40*(14), 2925–2934. https://doi.org/10.1523/JNEUROSCI.2048-19.2020

Bramson, B., Jensen, O., Toni, I., & Roelofs, K. (2018). Cortical Oscillatory Mechanisms Supporting the Control of Human Social–Emotional Actions. *The Journal of Neuroscience*, *38*(25), 5739–5749. https://doi.org/10.1523/JNEUROSCI.3382-17.2018

Brown, E. M., Pierce, M. E., Clark, D. C., Fischl, B. R., Iglesias, J. E., Milberg, W. P., McGlinchey, R. E., & Salat, D. H. (2020). Test-retest reliability of FreeSurfer automated hippocampal subfield segmentation within and across scanners. *NeuroImage*, *210*(August 2019), 116563. https://doi.org/10.1016/j.neuroimage.2020.116563

Chang, H., Shaw, D. S., & Cheong, J. (2015). The Development of Emotional and Behavioral Control in Early Childhood:Heterotypic Continuity and Relations to Early School Adjustment. *Journal of Child and Adolescent Behaviour*, *03*(03). https://doi.org/10.4172/2375-4494.1000204

Conty, L., & Grèzes, J. (2012). Look at me, I'll remember you: The Perception of Self-Relevant Social Cues Enhances Memory and Right Hippocampal Activity. *Human Brain Mapping*, *33*(10), 2428–2440. https://doi.org/10.1002/hbm.21366

Dale, A. M., Fischl, B., & Sereno, M. I. (1999). Cortical Surface-Based Analysis: I. Segmentation and Surface Reconstruction. *NeuroImage*, *9*(2), 179–194. https://doi.org/10.1006/NIMG.1998.0395

Dale, A. M., & Sereno, M. I. (1993). Improved Localizadon of Cortical Activity by Combining EEG and MEG with MRI Cortical Surface Reconstruction: A Linear Approach. *Journal of Cognitive Neuroscience*, *5*(2), 162–176. https://doi.org/10.1162/JOCN.1993.5.2.162

Dienes, Z. (2016). How Bayes factors change scientific practice. *Journal of Mathematical Psychology*, *72*, 78–89. https://doi.org/10.1016/j.jmp.2015.10.003

Fischl, B., & Dale, A. M. (2000). Measuring the thickness of the human cerebral cortex from magnetic resonance images. *Proceedings of the National Academy of Sciences*, *97*(20), 11050–11055. https://doi.org/10.1073/PNAS.200033797

Fischl, B., Liu, A., & Dale, A. M. (2001). Automated manifold surgery: Constructing geometrically accurate and topologically correct models of the human cerebral cortex. *IEEE Transactions on Medical Imaging*, *20*(1), 70–80. https://doi.org/10.1109/42.906426

Fischl, B., Salat, D. H., Busa, E., Albert, M., Dieterich, M., Haselgrove, C., Van Der Kouwe, A., Killiany, R., Kennedy, D., Klaveness, S., Montillo, A., Makris, N., Rosen, B., & Dale, A. M. (2002). Whole Brain Segmentation: Automated Labeling of Neuroanatomical Structures in the Human Brain. *Neuron*, *33*(3), 341–355. https://doi.org/10.1016/S0896-6273(02)00569-X

Fischl, B., Salat, D. H., Van Der Kouwe, A. J. W., Makris, N., Ségonne, F., Quinn, B. T., & Dale, A. M. (2004). Sequence-independent segmentation of magnetic resonance images. *NeuroImage*, *23*(SUPPL. 1), S69–S84. https://doi.org/10.1016/J.NEUROIMAGE.2004.07.016

Fischl, B., Sereno, M. I., & Dale, A. M. (1999). Cortical Surface-Based Analysis: II: Inflation, Flattening, and a Surface-Based Coordinate System. *NeuroImage*, *9*(2), 195–207. https://doi.org/10.1006/NIMG.1998.0396

Fischl, B., Sereno, M. I., Tootell, R. B. H., & Dale, A. M. (1999). High-Resolution Intersubject Averaging and a Coordinate System for the Cortical Surface. *Hum. Brain Mapping*, *8*, 272–284. https://doi.org/10.1002/(SICI)1097-0193(1999)8:4

Fischl, B., van der Kouwe, A., Destrieux, C., Halgren, E., Ségonne, F., Salat, D. H., Busa, E., Seidman, L. J., Goldstein, J., Kennedy, D., Caviness, V., Makris, N., Rosen, B., & Dale, A. M. (2004). Automatically Parcellating the Human Cerebral Cortex. *Cerebral Cortex*, *14*(1), 11–22. https://doi.org/10.1093/CERCOR/BHG087

Fuster, J. M. (2002). Frontal lobe and cognitive development. *Journal of Neurocytology*, *31*(3-5 SPEC. ISS.), 373–385. https://doi.org/10.1023/A:1024190429920

Giedd, J. N., Blumenthal, J., Jeffries, N. O., Castellanos, F. X., Liu, H., Zijdenbos, A., Paus, T., Evans, A. C., & Rapoport, J. L. (1999). Brain development during childhood and adolescence: A longitudinal MRI study. *Nature Neuroscience*, *2*(10), 861–863. https://doi.org/10.1038/13158

Han, X., Jovicich, J., Salat, D., van der Kouwe, A., Quinn, B., Czanner, S., Busa, E., Pacheco, J., Albert, M., Killiany, R., Maguire, P., Rosas, D., Makris, N., Dale, A., Dickerson, B., & Fischl, B. (2006). Reliability of MRI-derived

measurements of human cerebral cortical thickness: The effects of field strength, scanner upgrade and manufacturer. *NeuroImage*, *32*(1), 180–194. https://doi.org/10.1016/J.NEUROIMAGE.2006.02.051

Harooni, H. E., Naghdi, N., Sepehri, H., & Rohani, A. H. (2008). Intra hippocampal injection of testosterone impaired acquisition, consolidation and retrieval of inhibitory avoidance learning and memory in adult male rats. *Behavioural Brain Research*, *188*(1), 71–77. https://doi.org/10.1016/j.bbr.2007.10.017

Iglesias, J. E., Augustinack, J. C., Nguyen, K., Player, C. M., Player, A., Wright, M., Roy, N., Frosch, M. P., McKee, A. C., Wald, L. L., Fischl, B., & Van Leemput, K. (2015). A computational atlas of the hippocampal formation using ex vivo, ultra-high resolution MRI: Application to adaptive segmentation of in vivo MRI. *NeuroImage*, *115*, 117–137. https://doi.org/10.1016/j.neuroimage.2015.04.042

Ito, R., & Lee, A. C. H. (2016). The role of the hippocampus in approach-avoidance conflict decision-making: Evidence from rodent and human studies. *Behavioural Brain Research*, *313*, 345–357. https://doi.org/10.1016/j.bbr.2016.07.039

Jeffreys, H. (1939). *The Theory of Probability*. England: Oxford University Press. https://books.google.nl/books?hl=en&lr=&id=vh9Act9rtzQC&oi=fnd&pg=PA1&dq=jeffreys+1939+The+theory+of+probability&ots=ffRBGT32jS&sig=6AD3G2DUncJEKOx_zpEIMbOyc-k&redir_esc=y#v=onepage&q=jeffreys 1939 The theory of probability&f=false

Jenkinson, M., Beckmann, C. F., Behrens, T. E. J., Woolrich, M. W., & Smith, S. M. (2012). FSL. *NeuroImage*, *62*(2), 782–790. https://doi.org/10.1016/J.NEUROIMAGE.2011.09.015

Joormann, J., & Gotlib, I. H. (2010). Emotion regulation in depression: Relation to cognitive inhibition. *Cognition and Emotion*, *24*(2), 281–298. https://doi.org/10.1080/02699930903407948

Jovicich, J., Czanner, S., Greve, D., Haley, E., Van Der Kouwe, A., Gollub, R., Kennedy, D., Schmitt, F., Brown, G., MacFall, J., Fischl, B., & Dale, A. (2006). Reliability in multi-site structural MRI studies: Effects of gradient non-linearity correction on phantom and human data. *NeuroImage*, *30*(2), 436–443. https://doi.org/10.1016/J.NEUROIMAGE.2005.09.046

Kaldewaij, R., Koch, S. B. J., Zhang, W., Hashemi, M. M., Klumpers, F., & Roelofs, K. (2019a). Frontal Control Over Automatic Emotional Action Tendencies Predicts Acute Stress Responsivity. *Biological Psychiatry: Cognitive Neuroscience and Neuroimaging*, *4*(11), 975–983. https://doi.org/10.1016/j.bpsc.2019.06.011

Kaldewaij, R., Koch, S. B. J., Zhang, W., Hashemi, M. M., Klumpers, F., & Roelofs, K. (2019b). High Endogenous Testosterone Levels Are Associated With Diminished Neural Emotional Control in Aggressive Police Recruits. *Psychological Science*, *30*(8), 1161–1173. https://doi.org/10.1177/0956797619851753

Karalis, N., Dejean, C., Chaudun, F., Khoder, S., R Rozeske, R., Wurtz, H., Bagur, S., Benchenane, K., Sirota, A., Courtin, J., & Herry, C. (2016). 4-Hz oscillations synchronize prefrontal-amygdala circuits during fear behavior. *Nature Neuroscience*, *19*(4), 605–612. https://doi.org/10.1038/nn.4251

Kass, R. E., & Raftery, A. E. (1995). Bayes factors. *Journal of the American Statistical Association*, *90*(430), 773–795. https://doi.org/10.1080/01621459.1995.10476572

Kim, T., Hendrich, K., & Kim, S.-G. (2008). Functional MRI with magnetization transfer effects: Determination of BOLD and arterial blood volume changes. *Magnetic Resonance in Medicine*, *60*(6), 1518–1523. https://doi.org/10.1002/MRM.21766

Klein, A. M., Becker, E. S., & Rinck, M. (2011). Approach and Avoidance Tendencies in Spider Fearful Children: The Approach-Avoidance Task. *Journal of Child and Family Studies*, *20*(2), 224–231. https://doi.org/10.1007/s10826-010-9402-7

Laurita, A. C., & Spreng, R. N. (2017). The hippocampus and social cognition. In *The Hippocampus from Cells to Systems: Structure, Connectivity, and Functional Contributions to Memory and Flexible Cognition* (pp. 537–558). https://doi.org/10.1007/978-3-319-50406-3_17

LeGates, T. A., Kvarta, M. D., Tooley, J. R., Francis, T. C., Lobo, M. K., Creed, M. C., & Thompson, S. M. (2018). Reward behaviour is regulated by the strength of hippocampus–nucleus accumbens synapses. *Nature*, *564*(7735), 258–262. https://doi.org/10.1038/s41586-018-0740-8

Lu, H., & van Zijl, P. C. M. (2012). A review of the development of Vascular-Space-Occupancy (VASO) fMRI. *NeuroImage*, *62*(2), 736–742. https://doi.org/10.1016/j.neuroimage.2012.01.013

Lund, T. E., Nørgaard, M. D., Rostrup, E., Rowe, J. B., & Paulson, O. B. (2005). Motion or activity: Their role in intra- and inter-subject variation in fMRI. *NeuroImage*, *26*(3), 960–964. https://doi.org/10.1016/j.neuroimage.2005.02.021

Luo, Q., Misaki, M., Mulyana, B., Wong, C. K., & Bodurka, J. (2020). Improved autoregressive model for correction of noise serial correlation in fast fMRI. *Magnetic Resonance in Medicine*, *84*(3), 1293–1305. https://doi.org/10.1002/mrm.28203

MacLusky, N. J., Hajszan, T., Prange-Kiel, J., & Leranth, C. (2006). Androgen modulation of hippocampal synaptic plasticity. *Neuroscience*, *138*(3), 957–965. https://doi.org/10.1016/j.neuroscience.2005.12.054

Montagrin, A., Saiote, C., & Schiller, D. (2018). The social hippocampus. *Hippocampus*, *28*(9), 672–679. https://doi.org/10.1002/hipo.22797

Muscatell, K. A., Addis, D. R., & Kensinger, E. A. (2009). Self-involvement modulates the effective connectivity of the autobiographical memory network. *Social Cognitive and Affective Neuroscience*, *5*(1), 68–76. https://doi.org/10.1093/scan/nsp043

Neubert, F. X., Mars, R. B., Thomas, A. G., Sallet, J., & Rushworth, M. F. S. (2014). Comparison of Human Ventral Frontal Cortex Areas for Cognitive Control and Language with Areas in Monkey Frontal Cortex. *Neuron*, *81*(3), 700–713. https://doi.org/10.1016/j.neuron.2013.11.012

Olman, C. A., Davachi, L., & Inati, S. (2009). Distortion and signal loss in medial temporal lobe. *PLoS ONE*, *4*(12). https://doi.org/10.1371/journal.pone.0008160

Pitkänen, A., Pikkarainen, M., Nurminen, N., & Ylinen, A. (2000). Reciprocal connections between the amygdala and the hippocampal formation, perirhinal cortex, and postrhinal cortex in rat. *Annals of the New York Academy of Sciences*, *911*(1), 369–391. https://doi.org/10.1111/j.1749-6632.2000.tb06738.x

Reuter, M., Rosas, H. D., & Fischl, B. (2010). Highly accurate inverse consistent registration: A robust approach. *NeuroImage*, *53*(4), 1181–1196. https://doi.org/10.1016/J.NEUROIMAGE.2010.07.020

Roelofs, K., Minelli, A., Mars, R. B., van Peer, J., & Toni, I. (2009). On the neural control of social emotional behavior. *Social Cognitive and Affective Neuroscience*, *4*(1), 50–58. https://doi.org/10.1093/SCAN/NSN036

Roelofs, K., Putman, P., Schouten, S., Lange, W. G., Volman, I., & Rinck, M. (2010). Gaze direction differentially affects avoidance tendencies to happy and angry faces in socially anxious individuals. *Behaviour Research and Therapy*, *48*(4), 290–294. https://doi.org/10.1016/j.brat.2009.11.008

Rubin, R. D., Watson, P. D., Duff, M. C., & Cohen, N. J. (2014). The role of the hippocampus in flexible cognition and social behavior. *Frontiers in Human Neuroscience*, *8*(SEP), 742. https://doi.org/10.3389/fnhum.2014.00742

Saygin, Z. M., Kliemann, D., Iglesias, J. E., van der Kouwe, A. J. W., Boyd, E., Reuter, M., Stevens, A., Van Leemput, K., McKee, A., Frosch, M. P., Fischl, B., & Augustinack, J. C. (2017). High-resolution magnetic resonance imaging reveals nuclei of the human amygdala: manual segmentation to automatic atlas. *NeuroImage*, *155*, 370–382. https://doi.org/10.1016/J.NEUROIMAGE.2017.04.046

Schmelzeis, M. C., & Mittleman, G. (1996). The hippocampus and reward: Effects of hippocampal lesions on progressive-ratio responding. *Behavioral Neuroscience*, *110*(5), 1049–1066. https://doi.org/10.1037/0735-7044.110.5.1049

Schulz, J., Fazal, Z., Metere, R., Marques, J. P., & Norris, D. G. (2020). Arterial blood contrast (ABC) enabled by magnetization transfer (MT): a novel MRI technique for enhancing the measurement of brain activation changes. *BioRxiv*.

Schumacher, A., Villaruel, F. R., Ussling, A., Riaz, S., Lee, A. C. H., & Ito, R. (2018). Ventral Hippocampal CA1 and CA3 Differentially Mediate Learned Approach-Avoidance Conflict Processing. *Current Biology*, *28*(8), 1318-1324.e4. https://doi.org/10.1016/j.cub.2018.03.012

Schumacher, A., Vlassov, E., & Ito, R. (2016). The ventral hippocampus, but not the dorsal hippocampus is critical for learned approach-avoidance decision making. *Hippocampus*, *26*(4), 530–542. https://doi.org/10.1002/hipo.22542

Ségonne, F., Dale, A. M., Busa, E., Glessner, M., Salat, D., Hahn, H. K., & Fischl, B. (2004). A hybrid approach to the skull stripping problem in MRI. *NeuroImage*, *22*(3), 1060–1075. https://doi.org/10.1016/J.NEUROIMAGE.2004.03.032

Sosa, M., & Frank, L. M. (2018). Are We There Yet? Identification of Reward-Selective Cells in the Hippocampus. *Neuron*, *99*(1), 7–10. https://doi.org/10.1016/j.neuron.2018.06.037

Stein, J. L., Wiedholz, L. M., Bassett, D. S., Weinberger, D. R., Zink, C. F., Mattay, V. S., & Meyer-Lindenberg, A. (2007). A validated network of effective amygdala connectivity. *NeuroImage*, *36*(3), 736–745. https://doi.org/10.1016/j.neuroimage.2007.03.022

Toro-Serey, C., Tobyne, S. M., & McGuire, J. T. (2020). Spectral partitioning identifies individual heterogeneity in the functional network topography of ventral and anterior medial prefrontal cortex. *NeuroImage*, *205*, 116305. https://doi.org/10.1016/j.neuroimage.2019.116305

Tyborowska, A., Volman, I., Smeekens, S., Toni, I., & Roelofs, K. (2016). *Testosterone during Puberty Shifts Emotional Control from Pulvinar to Anterior Prefrontal Cortex*. https://doi.org/10.1523/JNEUROSCI.3874-15.2016

Tzschoppe, J., Nees, F., Banaschewski, T., Barker, G. J., Büchel, C., Conrod, P. J., Garavan, H., Heinz, A., Loth, E., Mann, K., Martinot, J. L., Smolka, M. N., Gallinat, J., Ströhle, A., Struve, M., Rietschel, M., Schumann, G., & Flor, H. (2014). Aversive learning in adolescents: Modulation by amygdala-prefrontal and amygdala-hippocampal connectivity and neuroticism. *Neuropsychopharmacology*, *39*(4), 875–884. https://doi.org/10.1038/npp.2013.287

van Peer, J. M., Roelofs, K., Rotteveel, M., van Dijk, J. G., Spinhoven, P., & Ridderinkhof, K. R. (2007). The effects of cortisol administration on approach-avoidance behavior: An event-related potential study. *Biological Psychology*, *76*(3), 135–146. https://doi.org/10.1016/j.biopsycho.2007.07.003

Verhagen, L., Grol, M. J., Dijkerman, H. C., & Toni, I. (2006). Studying visually-guided reach-to-grasp movements in an MR-environment. *NeuroImage*, *31*(S45).

Volman, I., Roelofs, K., Koch, S., Verhagen, L., & Toni, I. (2011). Anterior prefrontal cortex inhibition impairs control over social emotional actions. *Current Biology*, *21*(20), 1766–1770. https://doi.org/10.1016/j.cub.2011.08.050

Volman, I., Verhagen, L., den Ouden, H. E. M., Fernández, G., Rijpkema, M., Franke, B., Toni, I., & Roelofs, K. (2013). Reduced serotonin transporter availability decreases prefrontal control of the amygdala. *Journal of Neuroscience*, *33*(21), 8974–8979. https://doi.org/10.1523/JNEUROSCI.5518-12.2013

Volman, I., von Borries, A. K. L., Bulten, B. H., Verkes, R. J., Toni, I., & Roelofs, K. (2016). Testosterone modulates altered prefrontal control of emotional actions in psychopathic offenders. *ENeuro*, *3*(1), 52–60. https://doi.org/10.1523/ENEURO.0107-15.2016

Wisse, L. E. M., Daugherty, A. M., Olsen, R. K., Berron, D., Carr, V. A., Stark, C. E. L., Amaral, R. S. C., Amunts, K., Augustinack, J. C., Bender, A. R., Bernstein, J. D., Boccardi, M., Bocchetta, M., Burggren, A., Chakravarty, M. M., Chupin, M., Ekstrom, A., de Flores, R., Insausti, R., … la Joie, R. (2017). A harmonized segmentation protocol for hippocampal and parahippocampal subregions: Why do we need one and what are the key goals? *Hippocampus*, *27*(1), 3–11. https://doi.org/10.1002/hipo.22671

Wolff, S. D., & Balaban, R. S. (1989). Magnetization transfer contrast (MTC) and tissue water proton relaxation in vivo. *Magnetic Resonance in Medicine*, *10*(1), 135–144. https://doi.org/10.1002/MRM.1910100113

Yushkevich, P. A., Pluta, J. B., Wang, H., Xie, L., Ding, S. L., Gertje, E. C., Mancuso, L., Kliot, D., Das, S. R., & Wolk, D. A. (2015). Automated volumetry and regional thickness analysis of hippocampal subfields and medial temporal cortical structures in mild cognitive impairment. *Human Brain Mapping*, *36*(1), 258–287. https://doi.org/10.1002/hbm.22627

Zhou, J., Payen, J.-F., & Zijl, P. C. M. van. (2005). The interaction between magnetization transfer and blood-oxygen-level-dependent effects. *Magnetic Resonance in Medicine*, *53*(2), 356–366. https://doi.org/10.1002/MRM.20348

Appendix 1

Model employed for Behavioural analysis:

response + valence + gender + testosterone + cortisol + response*valence + response*gender + valence*gender + response*valence*gender

Neuroimaging-based model:

response + valence + CA + gender + testosterone + cortisol + response*valence + response*CA + response*gender + valence*CA + valence*gender + CA*gender + response*valence*CA + response*valence*gender + valence*CA*gender + response*valence*CA*gender

Appendix 2

Table 3: Bayesian statistical results from the behavioural and single-subject mixed-measures ANOVAs. The table includes the prior, posterior, and Bayes factor of all factors and interactions employed in the according models.

Analysis	Effects	P(incl)	P(incl|data)	BF(incl)
Reaction Times	Valence	0.737	0.19	0.084
	Response	0.737	0.164	0.07
	Gender	0.737	0.456	0.307
	Testosterone	0.5	0.181	0.221
	Cortisol	0.5	0.201	0.251
	Valence*Response	0.316	0.006	0.014
	Valence*Gender	0.316	0.021	0.047

	Response*Gender	0.316	0.015	0.034
	Valence*Response*Gender	0.053	$1.104e^{-4}$	0.002
Accuracy	Valence	0.737	0.824	1.677
	Response	0.737	0.814	1.566
	Gender	0.737	0.978	16.072
	Testosterone	0.5	0.278	0.386
	Cortisol	0.5	0.232	0.302
	Valence*Response	0.316	0.759	6.819
	Valence*Gender	0.316	0.230	0.648
	Response*Gender	0.316	0.172	0.449
	Valence*Response*Gender	0.053	0.014	0.318
CA's peak-voxel beta values	Valence	0.886	0.222	0.037
	Response	0.886	0.88	0.938
	CA	0.886	0.251	0.043
	Gender	0.886	0.6	0.193
	Testosterone	0.5	0.164	0.196
	Cortisol	0.5	0.207	0.261
	Valence*Response	0.503	0.071	0.075
	Valence*CA	0.503	0.1	0.01
	Valence*Gender	0.503	0.036	0.037
	Response*CA	0.503	0.034	0.034
	Response*Gender	0.503	0.518	1.062
	CA*Gender	0.503	0.023	0.024
	Valence*Response*CA	0.12	$1.069e^{-4}$	$7.856e^{-4}$
	Valence*Response*Gender	0.12	0.0016	0.122
	Valence*CA*Gender	0.12	$7.118e^{-4}$	$5.232e^{-4}$
	Response*CA*Gender	0.12	0.001	0.008
	Valence*Response*CA*Gender	0.006	$1.327e^{-7}$	$2.203e^{-5}$

Appendix 3

Figure 6: Significant correlation between testosterone and congruency scores within aPFC, BLA, and anterior hippocampal voxels

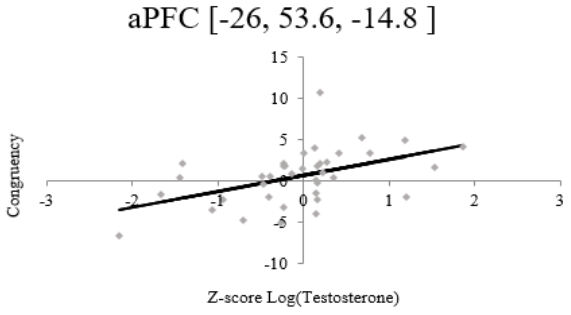

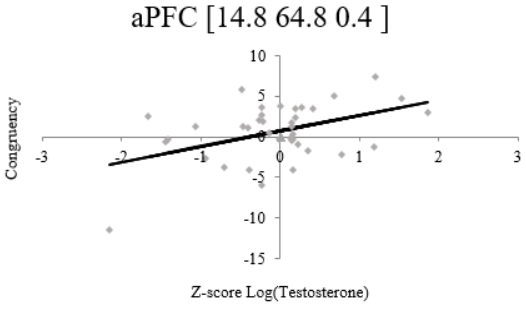

BLA [-18.8, -2.4, -14.8]

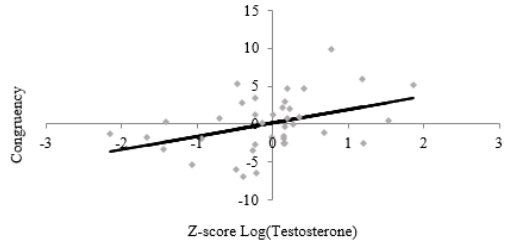

Hippocampus [-23.6, -17.6, -15.6]

Hippocampus [28.4, -12.8, -14.8]

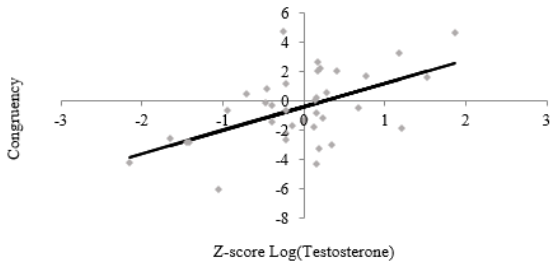

aPFC [-25.2 47.2 -0.4]

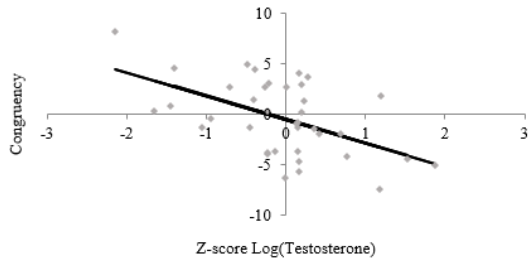

aPFC [35.6 52 2]

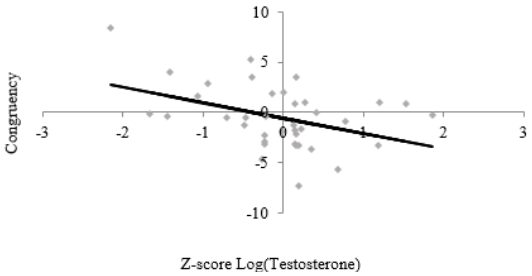

Hippocampus [25.2, -12.8, -22]

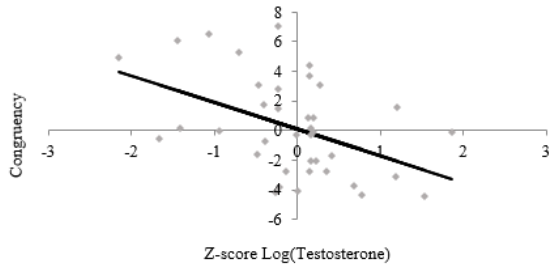

Hippocampus [-29.2, -8.8, -29.2]